

Research Article

Ventricular Dysfunction in Obese and Nonobese Rats with Metabolic Syndrome

Julian Torres-Jacome,¹ Brian Sabino Ortiz-Fuentes,¹ Daniela Bernabe-Sanchez,¹ Benjamin Lopez-Silva,¹ Myrian Velasco,² Martha Lucia Ita-Amador,³ and Alondra Albarado-Ibañez^{1,4}

¹Laboratorio de Fisiopatología Cardiovascular, Instituto de Ciencias, Benemérita Universidad Autónoma de Puebla, Puebla, Mexico

²Neuroscience Division, Instituto de Fisiología Celular, Department of Cognitive Neuroscience, Universidad Nacional Autónoma de México, México City, Mexico

³Laboratorio de Fisiopatología Cardiovascular, Complejo Nororiental, Benemérita Universidad Autónoma de Puebla, Puebla, Mexico

⁴Laboratorio de Aplicaciones Biotecnológicas, Instituto de Ciencias, Benemérita Universidad Autónoma de Puebla, Puebla, Mexico

Correspondence should be addressed to Alondra Albarado-Ibañez; a100102@hotmail.com

Received 15 November 2021; Revised 26 January 2022; Accepted 28 January 2022; Published 22 February 2022

Academic Editor: Ilias Migdalis

Copyright © 2022 Julian Torres-Jacome et al. This is an open access article distributed under the Creative Commons Attribution License, which permits unrestricted use, distribution, and reproduction in any medium, provided the original work is properly cited.

Obesity and dyslipidemias are both signs of metabolic syndrome, usually associated with ventricular arrhythmias. Here, we tried to identify cardiac electrical alteration and biomarkers in nonobese rats with metabolic syndrome (MetS), and these findings might lead to more lethal arrhythmias than obese animals. The MetS model was developed in Wistar rats with high-sucrose diet (20%), and after twenty-eight weeks were obtained two subgroups: obese (OMetS) and nonobese (NOMetS). The electrocardiogram was used to measure the ventricular arrhythmias and changes in the heart rate variability. Also, we measured ventricular hypertrophy and its relationship with electrical activity alterations of both ventricles, using micro-electrode and voltage clamp techniques. Also, we observed alterations in the contraction force of ventricles where a transducer was used to record mechanical and electrical papillary muscle, simultaneously. Despite both subgroups presenting long QT syndrome (0.66 ± 0.05 and 0.66 ± 0.07 ms with respect to the control 0.55 ± 0.1 ms), the changes in the heart rate variability were present only in OMetS, while the NOMetS subgroup presented changes in QT interval variability (NOMetS SD = 1.8, SD 2 = 2.8; SD1/SD2 = 0.75). Also, the NOMetS revealed tachycardia (10%; $p < 0.05$) with changes in action potential duration (63% in the right papillary and 50% in the left papillary) in the ventricular papillary which are correlated with certain alterations in the potassium currents and the force of contraction. The OMetS showed an increase in action potential duration and the force of contraction in both ventricles, which are explained as bradycardia. Our results revealed lethal arrhythmias in both MetS subgroups, irrespectively of the presence of obesity. Consequently, the NOMetS showed mechanical-electrical alterations regarding ventricle hypertrophy that should be at the NOMetS, leading to an increase of CV mortality.

1. Introduction

The MetS is known as a cluster of risk factors (impaired fasting glucose, insulin resistance, hypertension, dyslipidemias, and central obesity) [1–3] for type 2 diabetes mellitus and cardiovascular diseases, which occur together more often than by chance alone [4], that are associated with excess morbidity or/and mortality in humans [1, 5].

Obesity is a global epidemic for children [6] and adults, increasing the risk for cardiovascular morbidity and mortality, and the fact that obese along with overweight people are more prone to develop hypertension, hyperinsulinemia, dyslipidemias, and glucose homeostasis alteration [7–9].

The risk of development of cardiovascular diseases such as congestive heart failure, myocardial infarction, atrial fibrillation, and dilated cardiomyopathy is also increased [10, 11].

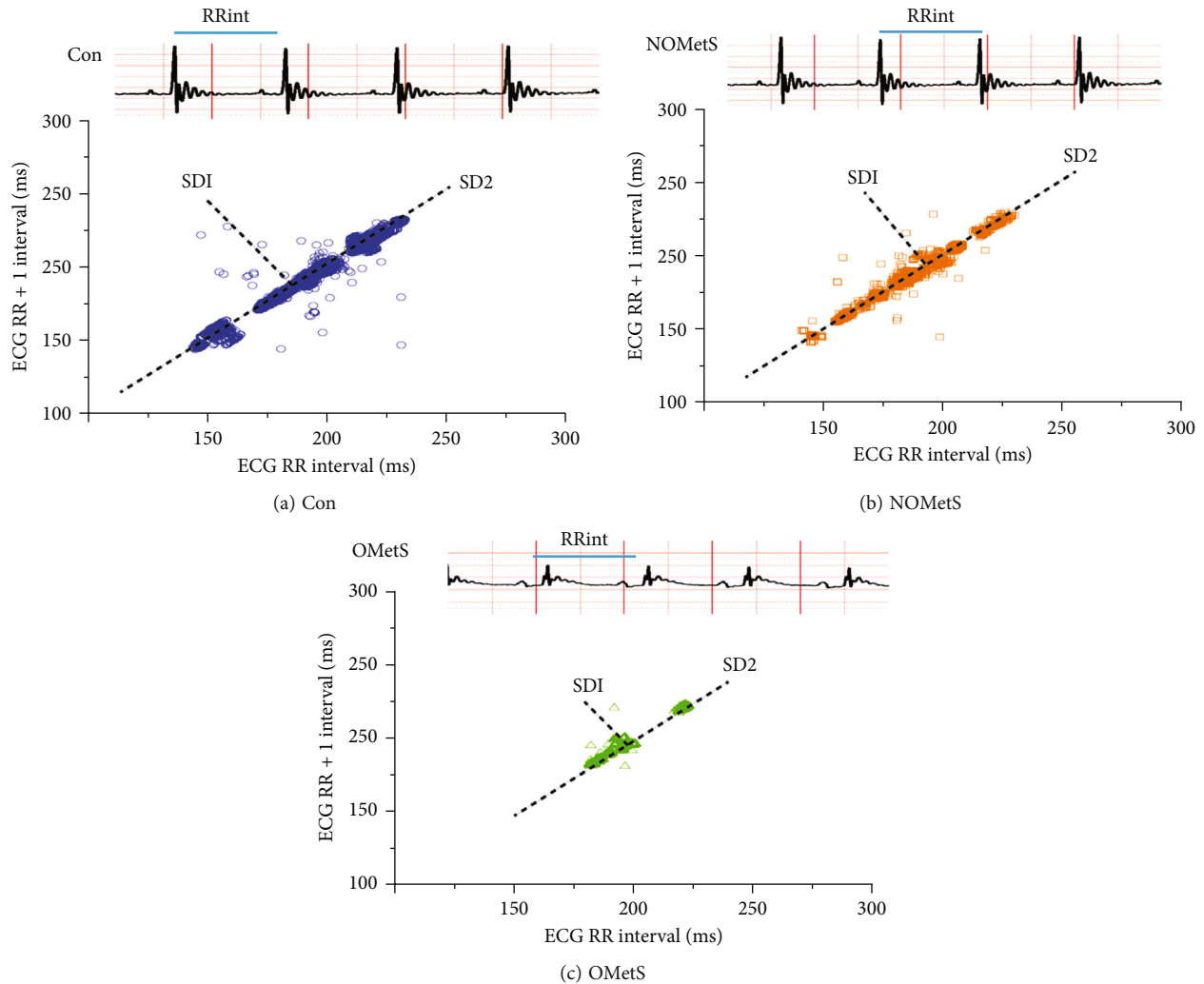


FIGURE 1

Generally, cardiomyopathy is commonly associated with electrocardiographic abnormalities [12], including impaired cardiac contractile [13]. Moreover, the long QT syndrome is related to alterations in ventricular electrical repolarization [14], and QT interval dispersion of ECG [15]. The alterations in beat-to-beat cardiac are clinically associated with cardiovascular risks [16]. One way of prognosis and diagnosis of cardiac diseases is to determine the heart rate variability (HRV) with the interval electrocardiogram (ECG) analysis [17]. On the other hand, the HRV is a noninvasive method that allows prognostic left ventricular dysfunction [18] and prolongation of QT intervals which are considered a factor risk to ventricular arrhythmias like Torsade de Pointes [17, 18]. Moreover, HRV is used to assess heart's health status at the prognosis, diagnosis of diabetes mellitus, hypertension, MetS, and obesity [19–21]. The relationship between lethal ventricular arrhythmias, cardiomyopathies, and LV dysfunction (associated with dyslipidemias and visceral fat) has been poorly identified and discussed in current literature [22, 23].

In this research, the MetS model gives us some information about the cardiomyopathies and lethal arrhythmias in obese and nonobese animal models. Our hypotheses is that

the NOMetS could show higher probability of more lethal arrhythmias than in OMetS, the NOMetS is not usually considered as a cardiac critical problem due to clinically confuse it the obesity is condition to dyslipidemias and cardiac electrical alterations. Consequently, we suggest that the quantification of blood plasma biochemistry and electrocardiogram analysis allowed us to know more about arrhythmias more than waist measure in subjects with MetS.

2. Material and Methods

2.1. Animal Model. All animal procedures were performed according to the International Guiding Principles for Biomedical Research Involving Animals Council for the International Organization of Medical Science 2010, including the Animal Ethics Committee of the Internal Council and the Animal Care Committee of the Instituto de Fisiología Celular at the Universidad Nacional Autónoma de México. Twenty young adult male Wistar rodents (250–280 g) were kept in a 12 h light/dark cycle. MetS was induced by feeding with standard rat chow, composed by laboratory rodent diet (LABDIET 5001) with 28.5% of protein, 13.5% of fat, and

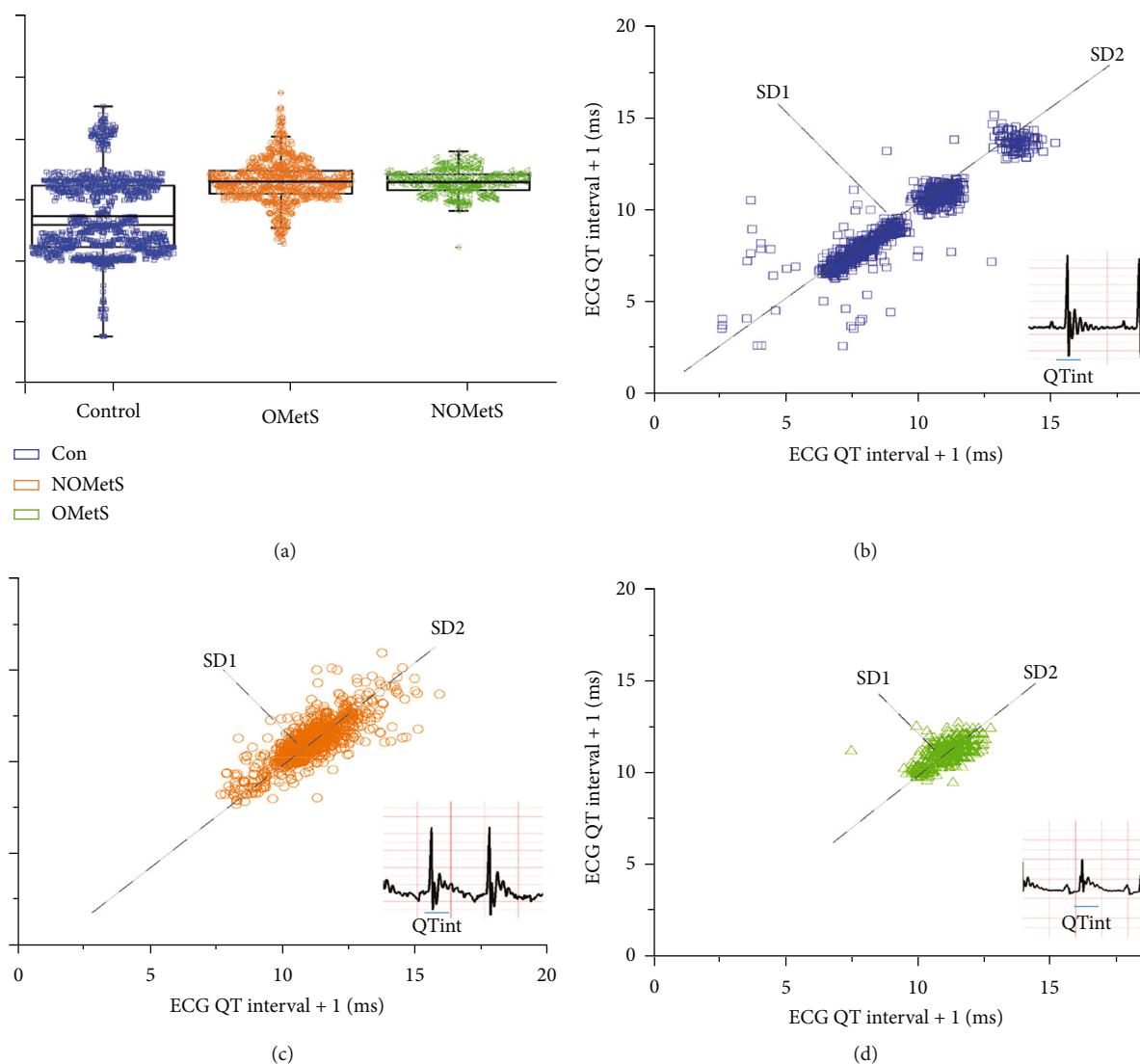


FIGURE 2

58% of carbohydrates [24]. Ad libitum tap water was provided to the control group and 20% (*w/v*) of sucrose solution to the experimental group for a twenty-eight-week treatment. The animals were anesthetized with an intraperitoneal sodium pentobarbital injection (40 mg/kg) [25]. The following measures were taken by abdominal circumference, epididymal fat, body weight, and body length. After, some blood peripancreatic and epididymal fat samples were taken, and then, the heart was removed. Finally, the animals were euthanized by cervical dislocation.

2.2. Biochemical Measurements. Peripheral venous blood samples were used to quantify glucose, insulin, triglycerides, and total cholesterol using standard laboratory techniques in 8-hour-fasted rats [26]. The insulin resistance (IR) was quantified via the homeostasis model assessment of HOMA $IR = \text{serum insulin (uUI/ml)} * (\text{blood glucose (mmol/L)}/22.5$ [27, 28].

2.3. Cardiac Function. The ECG was performed on anesthetized (0.5 mg/0.2 mg ketamine-xylazine/kg weight) rats. Bipolar ECGs were recorded using subcutaneous needle electrodes with Lead-I configuration; that signal was amplified in 700x and digitalized and captured to 10 kHz frequency for thirty minutes [25]. Data was stored in a personal computer and analyzed off-line, using Clampfit (molecular devices). All rats were continuously monitored to guarantee the right ventilation and temperature.

2.4. Ventricular Function. The heart was quickly removed and placed in a retrograde perfusion system, with Tyrode's solution at 36°C to wash the heart. In addition, excitation-contraction coupling was measured in the ventricular left and right papillary muscle isolates placed in a chamber to record simultaneously contraction force and action potential perfused with Tyrode's solution at 36°C, gassed with carbogen.

According to Frank-Starling's law [29], the contraction force was performed in the papillary muscles at Maxime

TABLE 1: Metabolic Characterization of animal model.

	Control (n = 20)	NOMeS (n = 14)	OMeS (n = 6)
Morphometric parameters			
Length (cm)	25.6 ± 0.2	25.7 ± 0.2	27.6 ± 0.5*
Waist (cm)	23.4 ± 0.7	24 ± 0.7	27.8 ± 0.6*
Weight (g)	518 ± 12	529 ± 5	725 ± 22* [†]
Epididymal fat (g)	4.6 ± 0.4	7.9 ± 0.5*	16.3 ± 2* [†]
Peripancreatic fat (g)	1.97 ± 0.5	2.1 ± 0.4	3.9 ± 0.8* [†]
BMI (kg·m ⁻³)	31 ± 0.6	31 ± 0.6	36 ± 0.1*
Clinical biochemistry values			
Glucose (mg·dl ⁻¹)	90 ± 2	104 ± 3*	112 ± 7*
Urea	39 ± 10.6	29 ± 9*	33 ± 8*
Triglycerides (mg·dl ⁻¹)	75 ± 7	153 ± 33*	116 ± 22*
Insulin (pM·l ⁻¹)	26 ± 0.02	27 ± 0.03	22 ± 0.04
HDL-c (mg·dl ⁻¹)	15 ± 2	31 ± 7*	23 ± 5* [†]
LDL-c (mg·dl ⁻¹)	21 ± 4	47 ± 14*	23 ± 5 [†]
HOMA-IR	0.8	1*	0.9*

Mean ± SD; $p \leq 0.05$, * vs control, [†] vs NOMeS.

longitude (Lmax). The action potential was recorded using the sharp microelectrodes of borosilicate (filled with 3 M KCl with a resistance of 25–35 M Ω). The signal was amplified with a WPI Duo 776 electrometer, digitalized (SCB-68 Quick references label, National Instruments), and analyzed using ClampFit (molecular devices) and Origin 7.0 (Southampton). The characterization of the action potential was measured with amplitude and the APD at 30 and 90% of the repolarization. The excitation-contraction coupling phenomenon was measured, using the time between the maximum voltage of the action potential and the maximum force of the contraction, including the delay between the start of the action potential with the start of the force of contraction [30].

2.5. Isolated Ventricular Cells from the Heart. Rat heart was cannulated through the aorta and perfused, according to the Langendorff method. Consequently, the heart was perfused in a recirculation mode for 8 minutes with collagenase, 28 mg/50 ml (Sigma Aldrich) and protease 1 mg/50 ml in solution in a Ca²⁺ free buffer. Finally, papillary muscle was mechanically dissociated in Kraft-Brüeh (KB) solution [31].

2.6. Alterations in Ventricular Electrical Activity. The patch-clamp technique was applied in the whole-cell configuration to record total currents; the patch pipettes had a resistance between 2 and 4 M Ω . The signal was captured at 5.4 kHz and amplified, digitalized (Heka), and stored on a personal computer. The cardiomyocytes were placed in a perfusion chamber in an inverted microscope (Nikon). Only Ca²⁺ tolerant rod-shaped right and left papillary cells were selected for this study.

TABLE 2: Heart rate variability.

	CON (n = 20)	NOMeS (n = 14)	OMeS (n = 6)
ECG RR interval			
SD1	1.03	1.04	0.51* [†]
SD2	1.31	1.53	0.74* [†]
SD1/SD2	0.79	0.68*	0.69*
ECG QT interval			
SD1	1.14	1.8*	1.5
SD2	1.5	2.8*	1.8
SD1/SD2	0.88	0.75*	0.89

Mean ± SD; $p \leq 0.05$, * vs control, [†] vs NOMeS.

2.7. Potassium Currents. The potassium current (I_k) was elicited from a holding potential of -80 mV by a square voltage pulse of -40 mV at 5 ms, and depolarizing pulses to membrane potential from -40 mV to 50 mV for 500 ms were applied with 10 mV increments at 2 seconds intervals [31].

2.8. Solutions. The Clampex program of the pClamp software controlled the current- and voltage-clamp experimental protocols. The solution using during voltage clamp experiments was a normal external solution (in mM NaCl, 136; KCl, 5.4; MgCl₂, 1; HEPES-Na, 10; CaCl₂, 1.8; dextrose, 11; pH adjusted to 7.4 with NaOH). The potassium currents were recorded with extracellular solution that containing (in mM) choline chloride, 136; MgCl₂, 1; HEPES-K⁺, 4; HEPES, 6; N-Methyl-D-glucamine, 6; CaCl₂, 0.1; CoCl₂, 0.5; and dextrose, 11; and it was adjusted with KOH to pH 7.4. The KB solution Isenberg & Klockner 1982 is the following composition (in mM): taurine, 10; glutamic acid, 70; creatine, 0.5; succinic acid, 5; dextrose, 10; KH₂PO₄, 10; KCl, 20; HEPES-K⁺, 10; and EGTA-K⁺, to adjust the pH to 7.4 with KOH [31]. The solutions to patch pipettes or internal solutions had the following composition (mM): 80 potassium aspartate, 10 KH₂PO₄, 1 MgSO₄, 7 H₂O, 40 KCl, 10 HEPES, 10 EGTA, 3 Na₂ATP, and 0.2 NaGTP; pH was adjusted to 7.3 with KOH.

2.9. Cardiac Histopathologic Alterations. The ventricular muscle was embedded in paraffin for 5 μ m, and cuts were done from the base to apex. After deparaffinization, the sections were stained with hematoxylin-eosin. The tissue samples were examined under a 40x microscope, and it was semiquantitatively analyzed with the Image J program.

2.10. Heart Rhythm Alterations. For analysis of the heart rate variability, we used the Poincare plot, in which the time series of ECG Intervals were plotted against the next value in a Cartesian coordinate system. In this research, the Poincare plots were constructed with RR and QT intervals of the recorded ECG, of all rat groups. The heart rate variability was quantified using the means of parameters SD1, SD2, and SD1/SD1 in each condition research [19].

2.11. Statistical Analysis. All data were analyzed using descriptive statistics and expressed as means ± SD (Origin Pro 2017 and Clampfit 10.7). If the results presented a normal distribution and equal variance, Student's unpaired *t*

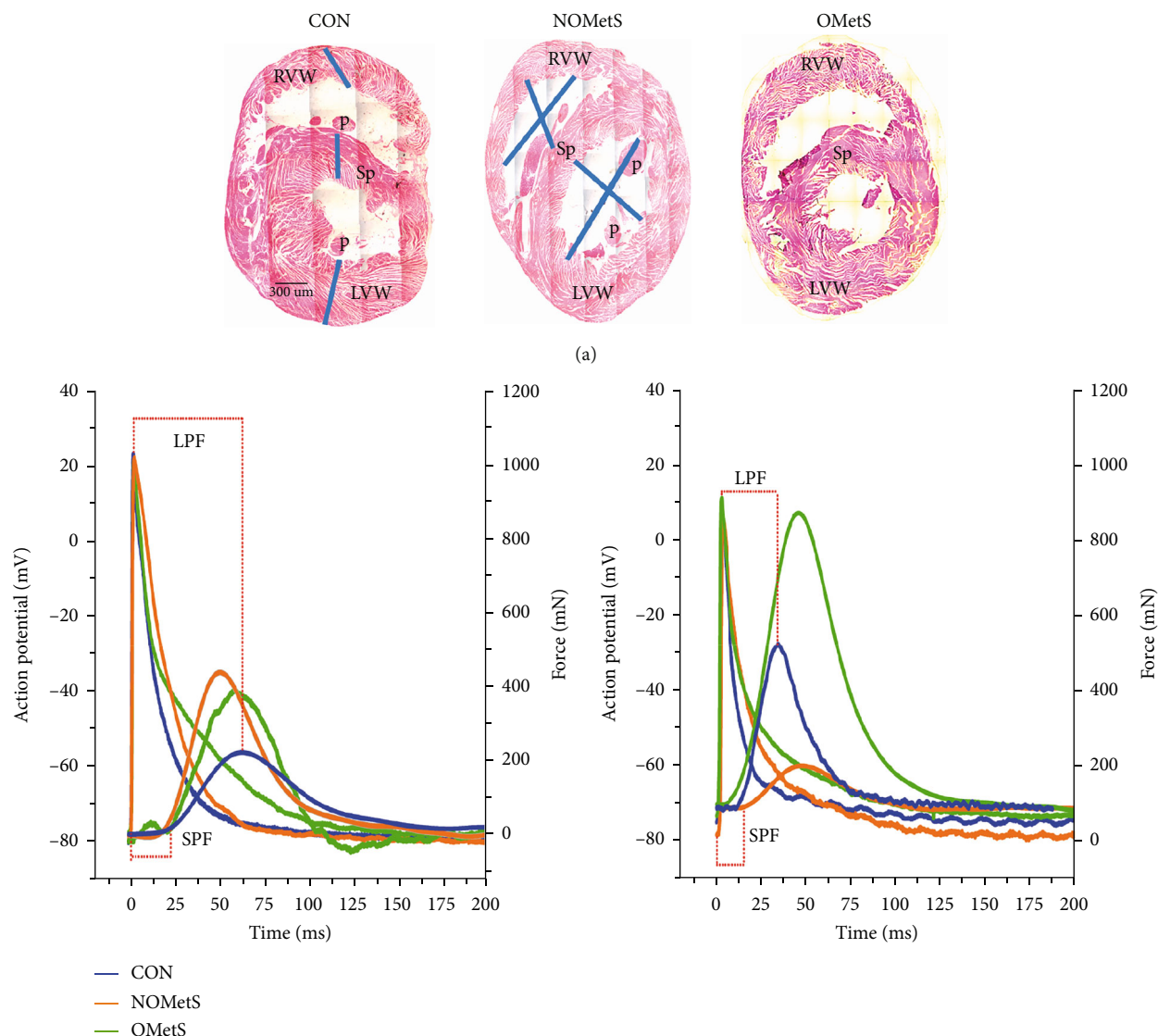


FIGURE 3

-test or one-way ANOVA was used by Dunnett's post hoc test. If the data presented a no-normal distribution or equal variance, the Mann-Whitney U test or Kruskal-Wallis test was performed. It was assumed to be a significant change if $p < 0.05$.

3. Results

3.1. Animal Model with Different Alterations in the Obesity of Metabolic Syndrome Profile. In the rodents, the high-sucrose diet by 24 weeks, developed MetS with three of the five metabolic (see Table 1) alterations as described by literature. In this model, seventy percent of those rats ($n = 14$) showed MetS with only a 2% body weight gain that is NOMetS, and this subgroup had the same abdominal circumference compared to the control group. However, these rats had 70% more epididymal fat than the control group. The

remaining rats with MetS ($n = 6$) showed a 40% body-weight gain, and OMetS were named as subgroups.

In the abdominal circumference and epididymis fat, a significant increase of 18% was detected in the NOMetS subgroup, while the value in the OMetS subgroup was 300%, compared to control. All Wistar rats with MetS presented alterations of lipid metabolism. Although, the data of NOMetS rats showed a significant increase in triglycerides (TG) levels compared to OMetS, 153 mg/dl and 116 mg/dl, as well as in c-LDL 47 mg/dl and 23 mg/dl respectively, see Table 1.

3.2. Effect of Obesity Profile on Heart Rhythm. The OMetS animal model presented a decrease of 308 ± 0.9 bpm in heart rate, while in the NOMetS subgroup, there was an increase of 330 ± 1 bpm compared to the control group which had 317 ± 0.5 bpm. Interestingly, the effect of obesity profile on the electrocardiogram record, in both cases NOMetS and

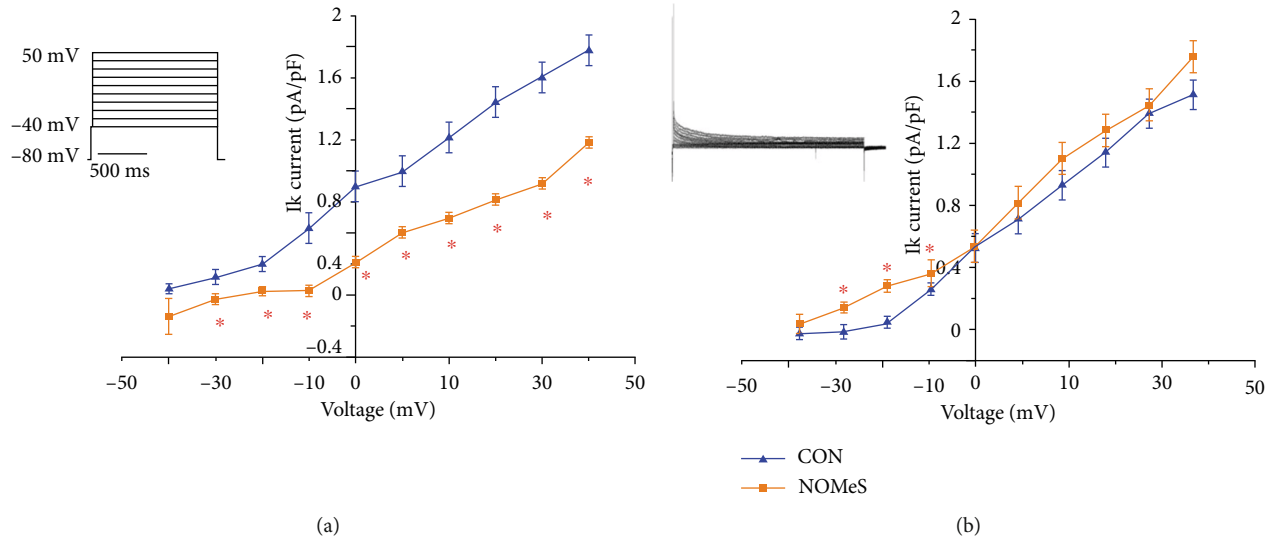


FIGURE 4

TABLE 3: Electrical and mechanical ventricular function.

	Control (n = 20)		NOMeS (n = 14)		OMeS (n = 6)	
	RPM	LPM	RPM	LPM	RPM	LPM
Amplitude (mV)	96 ± 2.4	87 ± 2	97 ± 1.6	91 ± 9	93 ± 2	79 ± 2*
APD 30% (ms)	6 ± 0.4	8 ± 0.8	6 ± 0.4	5.8 ± 0.4	7 ± 0.3*	7.4 ± 0.5
APD 90% (ms)	41 ± 1.8	38 ± 3	67 ± 4.4*	57 ± 2*	47 ± 2.7* [†]	70 ± 5.2*
LPF (ms)	57	73	56	50*	46*	49*
SPF (ms)	14	17	12	15*	12	10*
Force (mN)	311	477 [†]	519*	205*	615*	839* [†]

APD: action potential duration; LPM: left papillary muscle; RPM: right papillary muscle; LPF: latency period force; SPF: start period force. Mean ± SD; $p \leq 0.05$, * vs control, [†] vs NOMeS.

OMeS, was observed as in long QT syndrome; hence, the QTc values were longer 0.66 ± 0.05 and 0.66 ± 0.07 ms, respectively, than the control group, 0.55 ± 0.1 ms (Figures 1 and 2).

3.3. The Heart Rate Variability by Obesity. The cardiac health was evaluated with heart rate variability using Poincare plots, and as expected, the control group revealed an ellipse shape behavior (Figure 1(a)), with a variability of $SD1 = 1.03$, $SD2 = 1.31$, and index $SD1/SD2 = 0.79$ see Table 2. Together, in the data of heart rate variability of NOMeS rats, the ellipse shape is like the control group. Above the line identity of $SD2$ are registered the 80% of RR intervals, and $SD1/SD2$ index is decreased (Figure 1(b)). In the plot of OMeS subgroup, a decrease was observed in the heart rate variability in the $SD1$, $SD2$, and index $SD1/SD2$ biomarkers (see Figure 1(c)) compared with the control set (Table 2).

The beat-to-beat variations are also extremely sensitive to small fluctuations in several levels (Figure 2(a)). Thus, the variability in the QT intervals was quantified, which tends to behave in typical ellipse shape in the Poincare plots of RR interval (Figures 2(b)–2(d)). The quantitative analysis of the QT interval showed changes in the three biomarkers,

only in the OMeS subgroup (Table 2). The variability of the NOMeS subgroup had an increase in $SD1 = 1.8$, $SD2 = 2.8$, and the $SD1/SD2 = 0.75$ index (see Figure 2(c) and Table 2), meanwhile in the OMeS heart rate variability also increased, but not showing significant differences between aggregate sets (see Figure 2(d)).

3.4. Alterations in Ventricular Function Related to Obesity. Our results indicated that obesity profile altered the ventricular function, which was measured with excitation-contraction (E-C) coupling phenom. In the OMeS subgroup, the force contraction and action potential duration (APD) were higher in the left papillary ventricle than the right one. Consequently, E-C coupling was the desired outcome for ventricular function in the control rats (see Figure 3(b), Table 3). The NOMeS model showed alterations in the electrical and mechanical mechanisms of the E-C coupling. The contraction force increased 66 percent in the right and decreased 57 percent in the left papillary muscle while in relationship with the APD had an increased 61 percent and decreased 40 percent, respectively.

However, the left papillary muscle showed a decoupling which was related to the reduction in the latency period

(LPF) and the start period (SPF) of the contraction force (see Figure 3(b) and Table 3). The OMetS subgroup also presented an increase in the mechanisms of E-C coupling, showing a decoupled left papillary muscle of 30% and 40% in LPF and SPF, respectively, (Figures 3(a) and 3(b) and Table 3). The force was almost 2-fold than the control group.

High-sucrose diet-induced obesity is associated with hypertrophic cardiomyopathy [32]. The Hematoxylin-eosin staining (Figure 3(a)) suggests a ventricular hypertrophy in the NOMetS subgroup. The ventricles of the heart had a perimeter of 7.5 ± 0.5 mm, 6.5 ± 0.3 mm, and 4.6 ± 0.3 mm for NOMetS, OMetS, and control, respectively (Figure 3(a)). The MetS do not alter the ventricular-wall size, and the data showed 3.3 ± 1 , 2.8 ± 0.8 and 3.1 mm for NOMetS, OMetS, and control. Of note, there was no significant difference in heart weight, and the data were 2.1, 2.3 and 1.98 g for NOMetS, OMetS, and control, respectively.

3.5. The Obesity Profile Is Associated with Alterations in the Activity of Potassium Currents. The increase in APD of ventricles in NOMetS rats allowed indirectly induced changes in the potassium total currents. For this reason, we recorded potassium currents in isolated myocytes and the data showed a decrease in the amplitude of potassium current (Ito) in the right papillary muscle [33] (Figure 4(a)). Also, we measured the potassium current in myocytes of left papillary muscle; these currents showed an increase at only negative voltages (Figure 4(b)). Furthermore, the amplitude of each current component, obtained from the fitting, was normalized to cell capacitance to compare current densities from cells of different sizes. The NOMetS subgroup did not affect the resting membrane potential of ventricular papillary muscle (see Figure 4).

4. Discussion and Conclusions

This study proposed to identify cardiac electrical disease by electrical and metabolic biomarkers, using heart rate variability of RR, QT intervals, and blood plasma biochemistry to improve the diagnostic and prognosis of cardiometabolic diseases. Recent evidence suggests that genetic and environmental factors contribute to the MetS development; such factors are high-carbohydrates, high-fat diets, and lack of physical activity [24]. These factors promote insulin resistance, impaired fasting glucose, alteration of lipids metabolism, and a chronic inflammatory state and visceral obesity [34]. In this study, *Wistar* rats are not genetically susceptible to develop obesity [24]; though, a high-sucrose diet in drinking water like environmental factors produced MetS with resistance to insulin and dyslipidemia and impaired fasting glucose after 2 months of treatment [24]. In this model, after this twenty-eight-week high-sucrose diet, the rats presented MetS with and without obesity [35]. During a period of high-sucrose diet intake in the animal model, the liver tissue converted glucose into fatty acids and stored them in the adipose tissue [8, 36]. Consequently, in this study, both subgroups had increased in the distribution of epididymal fat weight by 0.7 and 2.5 times for NOMetS and OMetS, respectively (see Table 1). The NOMetS rats were showing insulin resistance, and this data

indicated in the rats a behavior of excess nutrients in their metabolism. This suggests an imbalance in the storage and synthesis of lipids in the liver, and the TG concentration in plasma is higher than control and OMetS [37]. Also, the NOMetS group had c-LDL and c-HDL plasma concentration higher than OMetS, and both proteins respond to the mechanism of high blood lipid metabolism and low reservoir in fat tissue [5]. These results explain that the rats with obesity only had the mechanism to reverse cholesterol transport [5].

The excess of fatty acids in plasma and insulin resistance has been proposed as a key driver for accumulation in obese individuals [2, 38]. In the MetS, the overweight model or OMetS under the higher-sucrose diet was enough to have an excess of triglycerides in plasma but c-HDL and insulin, similarly, in the control set. Furthermore, this model had alterations in HOMA-IR index [27] and the peripancreatic and epididymal fat increasing in 3 times and 85%, respectively, more than the control group. In general, obesity has been associated with the left ventricular dysfunction and cardiomyopathies by ventricular hypertrophy [39, 40].

However, the OMetS subjects only showed the electro-mechanical alterations in the function of both ventricles due to obesity. The outcomes revealed long QT syndrome related to alterations in the duration of AP ventricular and changes in the dispersion in RR. Also, the OMetS subgroup had alterations in the function of both ventricles (Figures 3(a) and 3(b). Table 3) and bradycardia, and the ventricle force augmented without alterations in ventricular morphology (Figure 3(b)).

On the other hand, the NOMetS subgroup presented syndrome long-QT with an increase in APD 90% in both chambers even without obesity, and it is worth mentioning that the clinical biomarkers of dyslipidemia and obesity were higher than that of the obese subgroup. The beginning of the QRS complex has been defined by the onset of ventricular electrical activity; the NOMetS. Also, this subgroup showed dispersion in QT intervals. This is related to susceptibility to reentry ventricular tachyarrhythmias and, revealed dysfunction in both ventricles, the contraction force was reduced in left papillary muscle, and the right papillary was enhanced, these alterations are caused by the changes to the electrical activity. Furthermore, the dispersion in electrical activity, at the start, the repolarization of action potential and the electro-mechanical changes allowed us to provoke the long QT syndrome in these animals [41].

On the other hand, the excitation-contraction decoupling was associated with hypertrophy [42]. In this model, the animals were fed with high sucrose diet and only the NOMetS subgroup presented eccentric hypertrophy associated with over ventricular dysfunction and fat tissue (see Table 1). These were related to the release of catecholamines in the heart [43]. Additionally, in NOMetS subgroup, tachycardia was observed, which is related to a parasympathetic innervation increase of pacemaker tissue [25].

The events that occur in E-C coupling of cardiac muscle depend on calcium concentration and the duration of action potential [44]. The lethal arrhythmia as the long QTc syndrome is correlated with APD prolongation, and the main cause is the reduction in the densities of K repolarizing

currents [45]. In the NOMetS animals, the alterations in the start and latency periods are presented, and an increase of APD associated with IK current decrease in the right ventricle [46] (see Figure 4).

In humans, the common central mechanisms modulated by both sympathetic and parasympathetic cardiovascular modulation were measured with HRV [47]. This biomarker is used to prognostic and diagnose health of the heart in metabolic diseases [48]. In this work, the HRV was impaired according to the levels of body fat, and the OMetS animals showed a decreased standard deviation in both mechanisms of modulation of the autonomic nervous system. The NOMetS animals presented an increase in the variability, only in QT intervals and the participation of the parasympathetic system (Figure 1(b)), raising the likelihood of lethal arrhythmias as long QT (Figure 2(a)), and the increase of modulation by the sympathetic and parasympathetic system on electrical properties of the ventricle (Figure 2(c)).

In this study, the c-HDL is high in both subgroups in which the protection was conferred to cardiovascular diseases [49] and attached to atherosclerosis [26]. However, both subgroups had high probability for lethal arrhythmias due to long QT syndrome and dyslipidemias (Table 1).

Additionally, the ventricular ejection force was measured with strain papillary muscle [42]; this data allowed indirectly to quantify the peripheral blood flow and ventricular chamber volumes [50]. The outcomes of the E-C coupling suggest that the left and right ventricles reflected alterations like cardiomyopathy in both MetS subgroups. The MetS with obesity did not alter morphologically the ventricles (Figure 3(a) and Table 3). Meanwhile, the H-E staining data revealed that the nonobese group exhibited a dilated cardiomyopathy [51]. The data showed the ventricular arrhythmias were produced by the MetS.

Finally, the type of ventricular arrhythmia depends on whether obesity is present or not. The outcomes suggest that the MetS without obesity promotes a poor prognosis of cardiomyopathies, and these alterations could be measured for prognostic and diagnostic purposes for the heart rate variability of ECG. The OMetS rats presented alterations of HRV with decreasing of asymmetry Poincare of RR interval, associated with increased contraction force in both ventricles and electrical alterations. However, the NOMetS animals had higher alterations in the metabolism, and the ventricular electrical activity are strongly correlated to long-QT syndrome, QT variability, and hypertrophic ventricular.

4.1. Statement Experimental Protocols. All animal procedures were performed in accordance with “International Guiding Principles for Biomedical Research Involving Animals”, Council for International Organization of Medical science 2010. The protocol was approved by the ethics committee (CICUAL-PROYECTO-00365) of the Benemérita Universidad Autónoma de Puebla.

Data Availability

The data sets used and/or analyzed during the current study are available from all authors on reasonable request.

Conflicts of Interest

The authors declare no competing interests.

Acknowledgments

The authors thank the support from Daniela Rodriguez Montaña IFC Histología UNAM, MVZ Héctor Malagon, and MVZ Daniel Garzón Biomédicas UNAM. We would like to acknowledge M. C. José Luis Carrillo Valdés Facultad de Lenguas-BUAP for discussing the manuscript in English.

References

- [1] B. O. Isomaa, P. Almgren, T. Tuomi et al., “Cardiovascular morbidity and mortality associated with the metabolic syndrome,” *Diabetes Care*, vol. 24, no. 4, pp. 683–689, 2001.
- [2] G. M. Reaven and Y. D. Chen, “Role of abnormal free fatty acid metabolism in the development of non-insulin-dependent diabetes mellitus,” *The American journal of medicine*, vol. 85, no. 5, pp. 106–112, 1988.
- [3] M. Cabral, S. I. Bangdiwala, M. Severo, J. T. Guimaraes, L. Nogueira, and E. Ramos, “Central and peripheral body fat distribution: different associations with low-grade inflammation in young adults?,” *Nutrition, Metabolism, and Cardiovascular Diseases: NMCD*, vol. 29, pp. 931–938, 2019.
- [4] K. G. Alberti, R. H. Eckel, S. M. Grundy et al., “Harmonizing the metabolic syndrome: a joint interim statement of the international diabetes federation task force on epidemiology and prevention; National Heart, Lung, and Blood Institute; American Heart Association; world heart federation; international atherosclerosis society; and International Association for the Study of obesity,” *Circulation*, vol. 120, pp. 1640–1645, 2009.
- [5] G. M. Reaven, C. Hollenbeck, C. Y. Jeng, M. S. Wu, and Y. D. Chen, “Measurement of plasma glucose, free fatty acid, lactate, and insulin for 24 h in patients with NIDDM,” *Diabetes*, vol. 37, no. 8, pp. 1020–1024, 1988.
- [6] A. Y. Chen, S. E. Kim, A. J. Houtrow, and P. W. Newacheck, “Prevalence of obesity among children with chronic conditions,” *Obesity*, vol. 18, pp. 210–213, 2010.
- [7] B. H. Goodpaster, S. Krishnaswami, T. B. Harris et al., “Obesity, regional body fat distribution, and the metabolic syndrome in older men and women,” *Archives of Internal Medicine*, vol. 165, no. 7, pp. 777–783, 2005.
- [8] J. M. de Jong, O. Larsson, B. Cannon, and J. Nedergaard, “A stringent validation of mouse adipose tissue identity markers,” *American Journal of Physiology. Endocrinology and Metabolism*, vol. 308, no. 12, pp. E1085–E1105, 2015.
- [9] L. J. van Loon and B. H. Goodpaster, “Increased intramuscular lipid storage in the insulin-resistant and endurance-trained state,” *Pflügers Archiv / European Journal of Physiology*, vol. 451, no. 5, pp. 606–616, 2006.
- [10] J. Qiu, H. Hu, S. Zhou, and Q. Liu, “Alteration of myocardium glucose metabolism in atrial fibrillation: cause or effect?,” *International Journal of Cardiology*, vol. 203, pp. 722–723, 2016.
- [11] M. Aurich, M. Niemers, P. Fuchs et al., “Pathophysiological background and prognostic implication of systolic aortic root motion in non-ischemic dilated cardiomyopathy,” *Scientific Reports*, vol. 9, p. 3866, 2019.

- [12] J. Zhang, F. Sacher, K. Hoffmayer et al., "Cardiac electrophysiological substrate underlying the ECG phenotype and electrogram abnormalities in Brugada syndrome patients," *Circulation*, vol. 131, no. 22, pp. 1950–1959, 2015.
- [13] C. X. Fang, F. Dong, D. P. Thomas, H. Ma, L. He, and J. Ren, "Hypertrophic cardiomyopathy in high-fat diet-induced obesity: role of suppression of forkhead transcription factor and atrophy gene transcription," *American Journal of Physiology. Heart and Circulatory Physiology*, vol. 295, no. 3, pp. H1206–H1215, 2008.
- [14] C. Jons, A. J. Moss, I. Goldenberg et al., "Risk of fatal arrhythmic events in long QT syndrome patients after syncope," *Journal of the American College of Cardiology*, vol. 55, pp. 783–788, 2010.
- [15] C. Madias, T. P. Fitzgibbons, A. A. Alsheikh-Ali et al., "Acquired long QT syndrome from stress cardiomyopathy is associated with ventricular arrhythmias and torsades de pointes," *Heart Rhythm*, vol. 8, pp. 555–561, 2011.
- [16] R. D. Lane, W. Zareba, H. T. Reis, D. R. Peterson, and A. J. Moss, "Changes in ventricular repolarization duration during typical daily emotion in patients with long QT syndrome," *Psychosomatic Medicine*, vol. 73, pp. 98–105, 2011.
- [17] K. McKechnie and A. Froese, "Ventricular tachycardia after ondansetron administration in a child with undiagnosed long QT syndrome," *Canadian journal of anaesthesia = Journal canadien d'anesthésie*, vol. 57, no. 5, pp. 453–457, 2010.
- [18] V. M. Phadumdeo and S. H. Weinberg, "Heart rate variability alters cardiac repolarization and electromechanical dynamics," *Journal of Theoretical Biology*, vol. 442, pp. 31–43, 2018.
- [19] R. E. Arroyo-Carmona, A. L. López-Serrano, A. Albarado-Ibañez et al., "Heart rate variability as early biomarker for the evaluation of diabetes mellitus progress," *Journal of Diabetes Research*, vol. 2016, 8483538 pages, 2016.
- [20] A. E. de Jong, E. Middelkoop, A. W. Faber, and N. E. Van Loey, "Non-pharmacological nursing interventions for procedural pain relief in adults with burns: a systematic literature review," *Burns: Journal of the International Society for Burn Injuries*, vol. 33, no. 7, pp. 811–827, 2007.
- [21] A. Laucyte-Cibulskiene, "Heart rate variability and pulse pressure amplification: lessons from diabetic patients," *Pulse*, vol. 5, pp. 125–126, 2018.
- [22] D. J. Lanska, M. J. Lanska, A. J. Hartz, R. K. Kalkhoff, D. Rupley, and A. A. Rimm, "A prospective study of body fat distribution and weight loss," *International Journal of Obesity*, vol. 9, pp. 241–246, 1985.
- [23] J. Liang, Y. Chen, J. Zhang et al., "Associations of weight-adjusted body fat and fat distribution with bone mineral density in Chinese children aged 6–10 years," *International Journal of Environmental Research and Public Health*, vol. 17, 2020.
- [24] C. Larqué, M. Velasco, V. Navarro-Tableros et al., "Early endocrine and molecular changes in metabolic syndrome models," *IUBMB Life*, vol. 63, pp. 831–839, 2011.
- [25] A. Albarado-Ibanez, J. E. Avelino-Cruz, M. Velasco, J. Torres-Jacome, and M. Hiriart, "Metabolic syndrome remodels electrical activity of the sinoatrial node and produces arrhythmias in rats," *PLoS One*, vol. 8, article e76534, 2013.
- [26] J. W. Jukema, A. H. Liem, P. H. Dunselman, J. A. van der Sloot, D. J. Lok, and A. H. Zwinderman, "LDL-C/HDL-C ratio in subjects with cardiovascular disease and a low HDL-C: results of the RADAR (rosuvastatin and atorvastatin in different doses and reverse cholesterol transport) study," *Current Medical Research and Opinion*, vol. 21, no. 11, pp. 1865–1874, 2005.
- [27] L. C. Antunes, J. L. Elkfury, M. N. Jornada, K. C. Foletto, and M. C. Bertoluci, "Validation of HOMA-IR in a model of insulin-resistance induced by a high-fat diet in Wistar rats," *Archives of endocrinology and metabolism*, vol. 60, pp. 138–142, 2016.
- [28] R. Ghiasi, F. Ghadiri Soufi, M. H. Somi et al., "Swim training improves HOMA-IR in type 2 diabetes induced by high fat diet and low dose of streptozotocin in male rats," *Advanced pharmaceutical bulletin*, vol. 5, no. 3, pp. 379–384, 2015.
- [29] A. V. Delicce and A. N. Makaryus, *Physiology, Frank Starling law*, StatPearls, Treasure Island (FL), 2020.
- [30] N. Kayhan, J. P. Bodem, C. F. Vahl, and S. Hagl, "The positive staircase (force-frequency relationship) and the Frank-Starling mechanism are altered in atrial myocardium of patients in end-stage heart failure transplanted for dilative cardiomyopathy," *Transplantation Proceedings*, vol. 34, pp. 2185–2191, 2002.
- [31] J. A. Sanchez-Chapula and M. C. Sanguinetti, "Altered gating of HERG potassium channels by cobalt and lanthanum," *Pflügers Archiv / European Journal of Physiology*, vol. 440, pp. 264–274, 2000.
- [32] P. J. Tucci, C. N. Faber, L. dos Santos, and E. L. Antonio, "Slow inotropic response of intact left ventricle to sudden dilation critically depends on a myocardial dialysable factor," *Clinical and Experimental Pharmacology & Physiology*, vol. 34, no. 5–6, pp. 515–516, 2007.
- [33] J. Torres-Jacome, M. Gallego, J. M. Rodriguez-Robledo, J. A. Sanchez-Chapula, and O. Casis, "Improvement of the metabolic status recovers cardiac potassium channel synthesis in experimental diabetes," *Acta Physiologica*, vol. 207, pp. 447–459, 2013.
- [34] J. A. Nazare, J. D. Smith, A. L. Borel et al., "Ethnic influences on the relations between abdominal subcutaneous and visceral adiposity, liver fat, and cardiometabolic risk profile: the international study of prediction of intra-abdominal adiposity and its relationship with cardiometabolic risk/intra-abdominal adiposity," *The American journal of clinical nutrition*, vol. 96, pp. 714–726, 2012.
- [35] G. A. Bray, "Fat distribution and body weight," *Obesity Research*, vol. 1, pp. 203–205, 1993.
- [36] P. Barter, "Managing diabetic dyslipidaemia—beyond LDL-C:HDL-C and triglycerides," *Atherosclerosis Supplements*, vol. 7, no. 4, pp. 17–21, 2006.
- [37] A. N. Mavrogiannaki and I. N. Migdalis, "Nonalcoholic fatty liver disease, diabetes mellitus and cardiovascular disease: newer data," *International Journal of Endocrinology*, vol. 2013, Article ID 450639, 2013.
- [38] J. M. Rantanen, S. Riahi, M. B. Johansen, E. B. Schmidt, and J. H. Christensen, "Effects of marine n-3x polyunsaturated fatty acids on heart rate variability and heart rate in patients on chronic dialysis: a randomized controlled trial," *Nutrients*, vol. 10, 2018.
- [39] A. Linhart and F. Cecchi, "Common presentation of rare diseases: left ventricular hypertrophy and diastolic dysfunction," *International Journal of Cardiology*, vol. 257, pp. 344–350, 2018.
- [40] J. K. Kirklin, "Predicting right ventricular failure after left ventricular assist device implantation: Frank and Starling prevail

- again,” *The Journal of Thoracic and Cardiovascular Surgery*, 2019.
- [41] S. Zicha, I. Moss, B. Allen et al., “Molecular basis of species-specific expression of repolarizing K⁺ currents in the heart,” *American Journal of Physiology. Heart and Circulatory Physiology*, vol. 285, pp. H1641–H1649, 2003.
- [42] B. O'Rourke, D. A. Kass, G. F. Tomaselli, S. Kaab, R. Tunin, and E. Marban, “Mechanisms of altered excitation-contraction coupling in canine tachycardia-induced heart failure, I: experimental studies,” *Circulation Research*, vol. 84, no. 5, pp. 562–570, 1999.
- [43] A. Albarado-Ibañez, R. E. Arroyo-Carmona, R. Sánchez-Hernández et al., “The role of the autonomic nervous system on cardiac rhythm during the evolution of diabetes mellitus using heart rate variability as a biomarker,” *Journal of Diabetes Research*, vol. 2019, 5157010 pages, 2019.
- [44] H. Kusuoka, Y. Koretsune, V. P. Chacko, M. L. Weisfeldt, and E. Marban, “Excitation-contraction coupling in postischemic myocardium. Does failure of activator Ca²⁺ transients underlie stunning?,” *Circulation Research*, vol. 66, pp. 1268–1276, 1990.
- [45] T. Aiba and W. Shimizu, “Molecular screening of long-QT syndrome: risk is there, or rare?,” *Heart Rhythm*, vol. 8, pp. 420–421, 2011.
- [46] J. Rose, A. A. Armoundas, Y. Tian et al., “Molecular correlates of altered expression of potassium currents in failing rabbit myocardium,” *American Journal of Physiology. Heart and Circulatory Physiology*, vol. 288, pp. H2077–H2087, 2005.
- [47] “Heart rate variability. Standards of measurement, physiological interpretation, and clinical use. Task force of the European Society of Cardiology and the north American Society of Pacing and Electrophysiology,” *European Heart Journal*, vol. 17, pp. 354–381, 1996.
- [48] R. Ö. Akbulak, S. C. Rosenkranz, B. N. Schaeffer et al., “Acute and long-term effects of fingolimod on heart rhythm and heart rate variability in patients with multiple sclerosis,” *Multiple Sclerosis and Related Disorders*, vol. 19, pp. 44–49, 2018.
- [49] L. R. Liu, J. F. Fu, L. Liang, and K. Huang, “Relationship between nonalcoholic fatty liver disease and cardiovascular disease in children with obesity,” *Zhongguo dang dai er ke za zhi = Chinese journal of contemporary pediatrics*, vol. 12, no. 7, pp. 547–550, 2010.
- [50] N. S. Schneider, T. Shimayoshi, A. Amano, and T. Matsuda, “Mechanism of the Frank-Starling law—a simulation study with a novel cardiac muscle contraction model that includes titin and troponin I,” *Journal of Molecular and Cellular Cardiology*, vol. 41, no. 3, pp. 522–536, 2006.
- [51] R. D. Berger, E. K. Kasper, K. L. Baughman, E. Marban, H. Calkins, and G. F. Tomaselli, “Beat-to-beat QT interval Variability,” *Circulation*, vol. 96, no. 5, pp. 1557–1565, 1997.